Electronic Supplementary Material (ESI) for Energy & Environmental Science.
This journal is © The Royal Society of Chemistry 2021

Supporting Information

Approaching a High-Rate and Sustainable Production of Hydrogen Peroxide: Oxygen Reduction on Co-N-C Single-Atom Electrocatalysts in Simulated Seawater

Qinglan Zhao,‡[a]* Yian Wang,‡[a] Wei-Hong Lai,‡[b] Fei Xiao,[a] Yuxiang Lyu,[a] Caizhi Liao,[c] and Minhua Shao[a,d]*

[a] *Department of Chemical and Biological Engineering, The Hong Kong University of Science and Technology, Clear Water Bay, Kowloon, Hong Kong, China.*

[b] *Institute for Superconducting & Electronic Materials, Innovation Campus, University of Wollongong, Wollongong, New South Wales, Australia.*

[c] *Creative Biosciences (Guangzhou) Co., Ltd., Guangzhou, 510535, China.*

[d] *Energy Institute, Hong Kong Branch of the Southern Marine Science and Engineering Guangdong Laboratory, and Chinese National Engineering Research Center for Control & Treatment of Heavy Metal Pollution, The Hong Kong University of Science and Technology, Clear Water Bay, Kowloon, Hong Kong, China.*

‡ These authors contributed equally to this work.

[*] *Email: keqzhao@ust.hk, kemshao@ust.hk*

Results

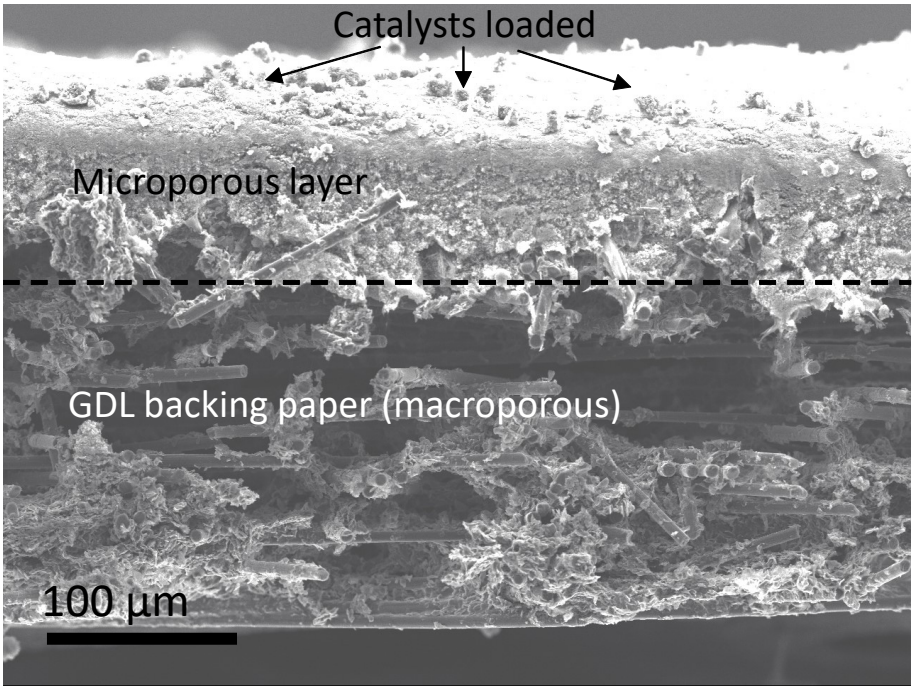

Figure S1. Cross-sectional scanning electron microscopy (SEM) image of Co-N-C catalysts on a Sigracet 39BB gas diffusion layer. (A catalyst loading of 2 mg cm^{-2} was sprayed on the carbon paper for a clearer image of catalyst distribution.)

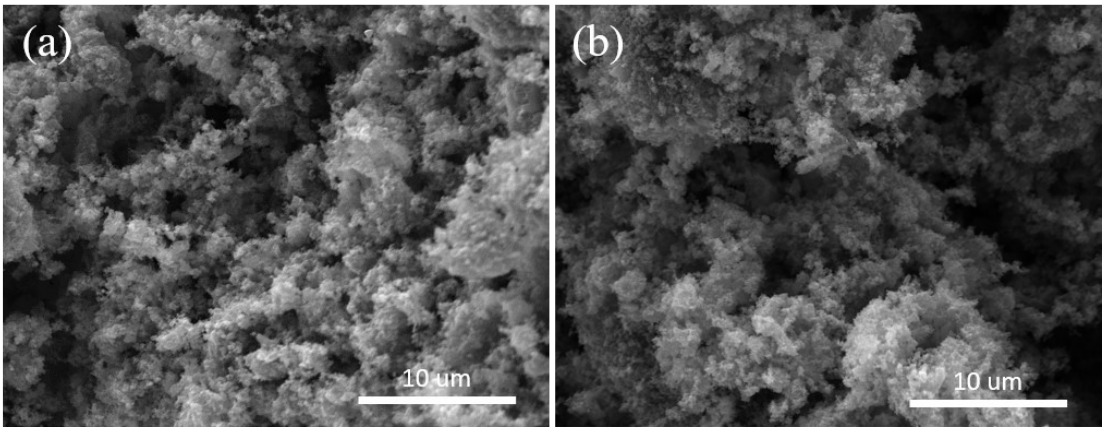

Figure S2. Scanning electron microscopy (SEM) images of (a) Co-N-C and (b) N-C samples.

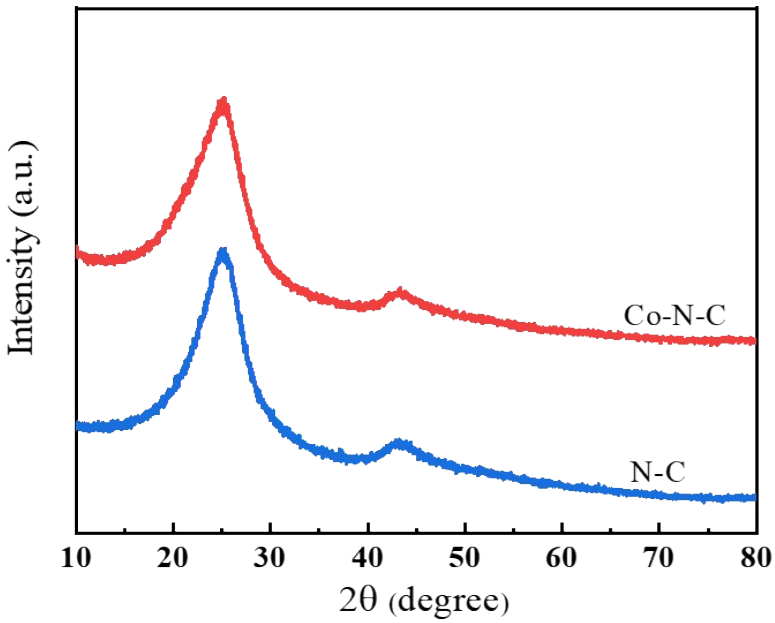

Figure S3. X-ray diffraction (XRD) patterns of the Co-N-C and N-C samples.

Table S1. Co content determined by X-ray photoelectron spectroscopy (XPS) and inductively coupled plasma mass spectrometry (ICP-MS).

Method	C	N	Co
XPS (at.%)	87.56	11.8	0.64
ICP-MS (wt.%)	-	-	0.97

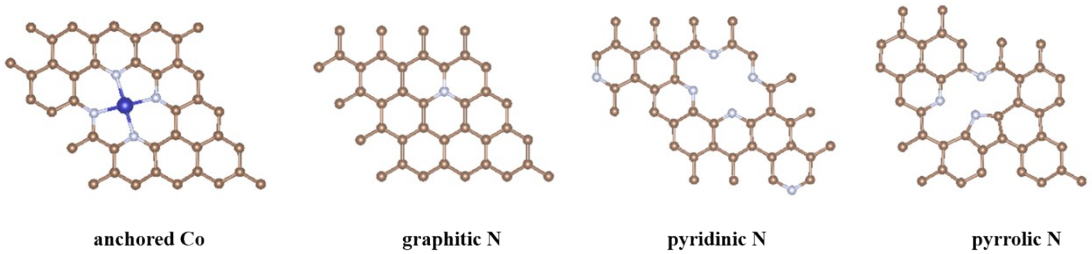

Figure S4. Top views of anchored Co, graphitic N, pyridinic N, and pyrrolic N.

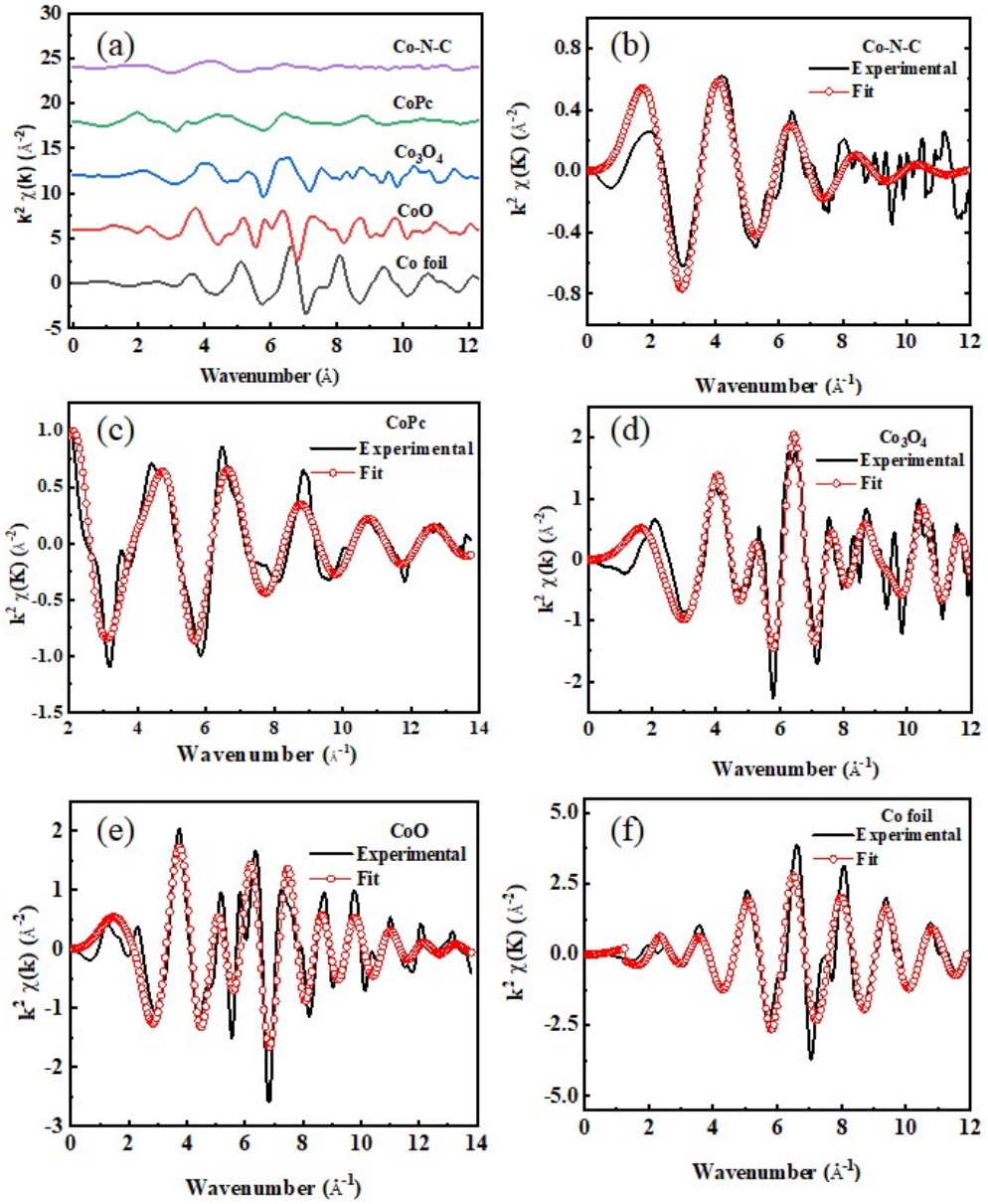

Figure S5. (a)k^2-weighted EXAFS spectra and (b-f) the corresponding fitting curves of Co-N-C, CoPc, Co_3O_4, CoO, and Co foil.

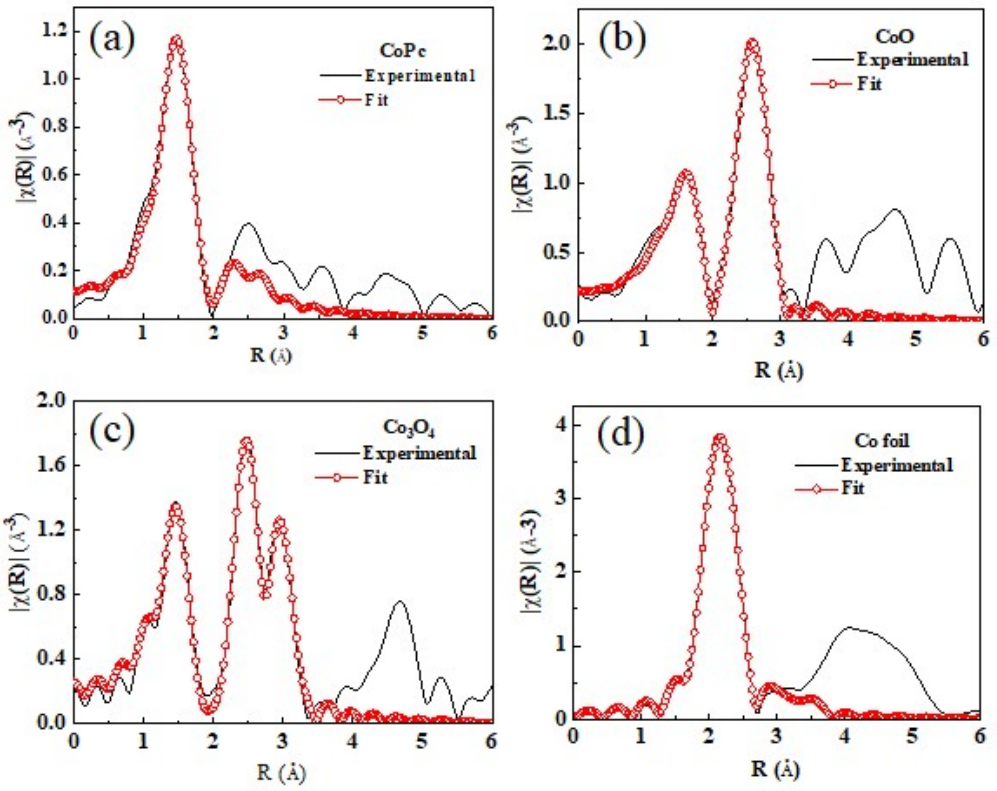

Figure S6. FT-EXAFS fitting curves of (a) CoPc, (b) CoO, (c) Co_3O_4, and (d) Co foil in R space.

Table S2. EXAFS fitting parameters at the Co K-edge for Co-N-C and standard samples.

	Path	**N**	**ΔE (eV)**	**100×R (Å)**	**100×σ² (Å ²)**	**R-factor**
Co foil	Co-Co	12.0	6.80 (0.51)	249.0 (0.3)	5.67 (0.43)	0.001
CoO	Co-O	6.0	-1.10 (2.08)	211.0 (1.9)	9.40 (1.71)	0.008
	Co-Co	12.0	-3.42 (1.19)	300.2 (0.9)	10.22 (0.90)	
	Co-O	5.3	-7.35 (1.46)	191.3 (0.8)	2.67 (0.69)	
Co_3O_4	Co-Co1	4.0	-7.72 (0.77)	285.3 (0.5)	2.54 (0.50)	0.005
	Co-Co2	9.3	-7.72 (0.77)	358.8 (0.7)	6.10 (0.62)	
CoPc	Co-N	4.0	5.46(1.12)	191.8(2.1)	3.92(0.46)	0.005
Co-N-C	Co-N	5.2 (0.70)	-3.72 (1.68)	197.4 (8.3)	11.28 (2.13)	0.008

The amplitude reduction factor S_0^2 was determined to be 0.72 through fitting the FT-EXAFS of standard Co foil which was measured simultaneously during the experiment. *N*, coordination number; Δ*E*, threshold energy correction; *R*, distance between absorber and backscatter atoms; σ^2, Debye-Waller factor to describe the variance due to disorder

(both lattice and thermal); the *R*-factor indicates the goodness of the fit.

Table S3. The range of the data used in the fitting for Co-N-C and standard samples in k-space and R-space.

Sample	k space	R space
Co foil	3.0≤k≤10.5	1≤R≤2.7
CoO	3.2≤k≤11.2	1≤R≤3.4
Co_3O_4	3.5≤k≤13.1	1≤R≤3.4
CoPc	3.0≤k≤10.6	1≤R≤2.2
Co-N-C	3.0≤k≤10.5	1≤R≤2.4

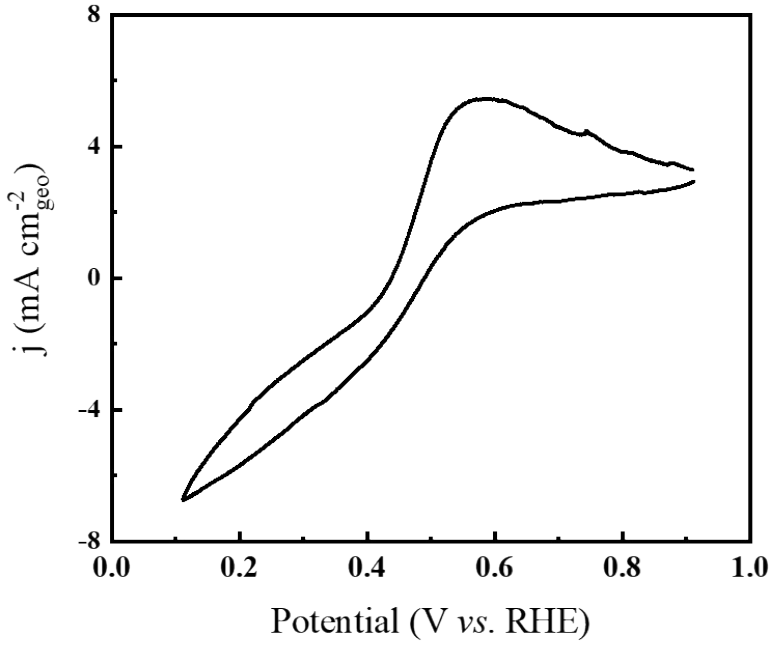

Figure S7. CV curve of Co-N-C catalyst in an N_2 saturated 0.5M NaCl containing 0.2M H_2O_2.

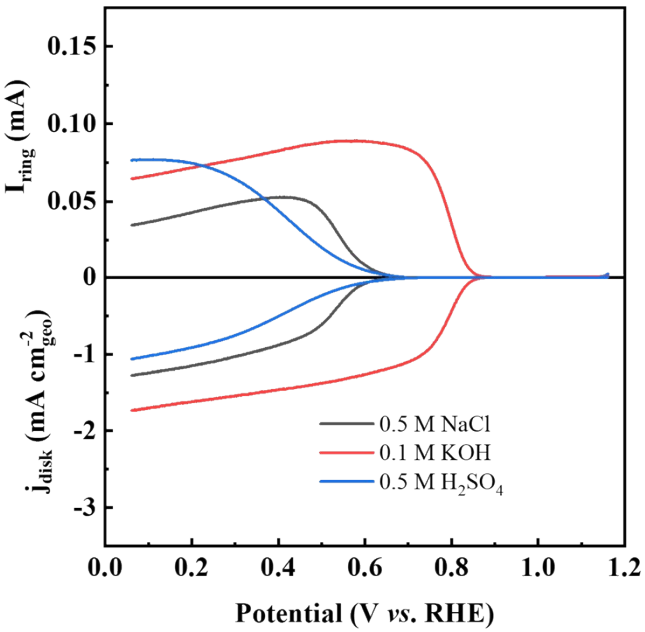

Figure S8. Linear sweep voltammetry (LSV) curves of Co-N-C at different electrolytes with various pH values in a RRDE setup with the ring current was collected on the Pt ring at a constant potential of +1.26 V_{RHE}.

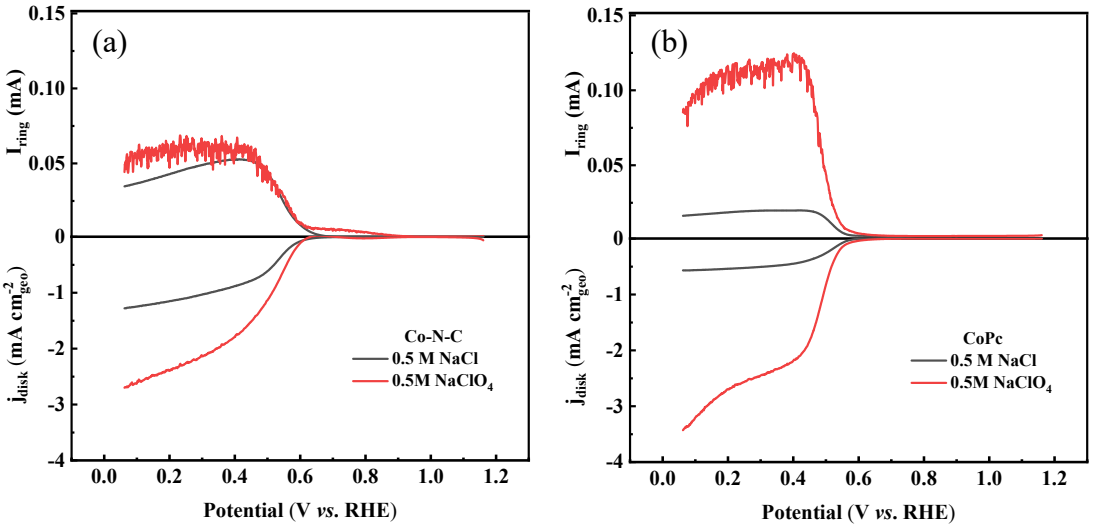

Figure S9. Linear sweep voltammetry (LSV) curves of (a) Co-N-C and (b) CoPc in 0.5M NaCl and 0.5M $NaClO_4$ in a RRDE setup with the ring current was collected on the Pt ring at a constant potential of +1.26 V_{RHE}.

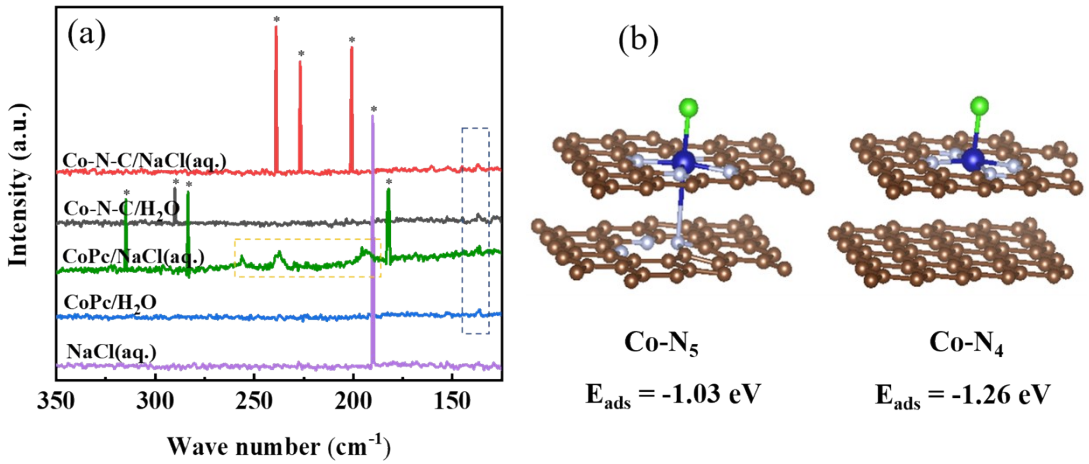

Figure S10. (a) Raman spectra of 0.5M NaCl and the interfaces between Co-N-C or CoPc and 0.5M NaCl or H_2O (* indicates signals from the environmental light), and (b) adsorption of chloride ion on Co-N_5 and Co-N_4 surfaces with adsorption energies (E_{ads}) computed by DFT (color notation: dark blue-Co, brown-C, light blue-N, green-Cl).

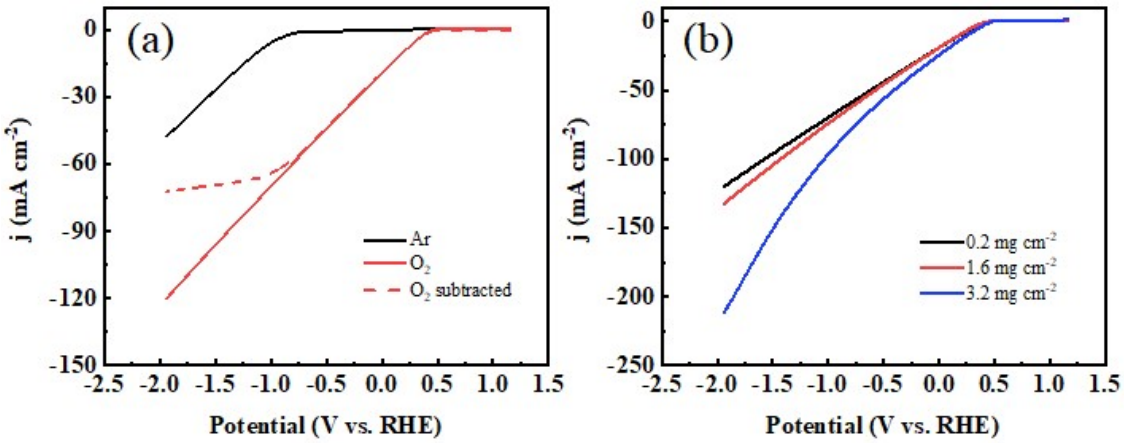

Figure S11. (a) LSV curves of Co-N-C cathode with a mass loading of 0.2 mg cm^{-2} in flow cell under the flow of O_2 and Ar (the red dash line was obtained by subtracting the current under the flow of Ar); (b) LSV curves of Co-N-C cathode with a mass loading of 0.2, 1.6, 3.2 mg cm^{-2} in flow cell under the flow of O_2.

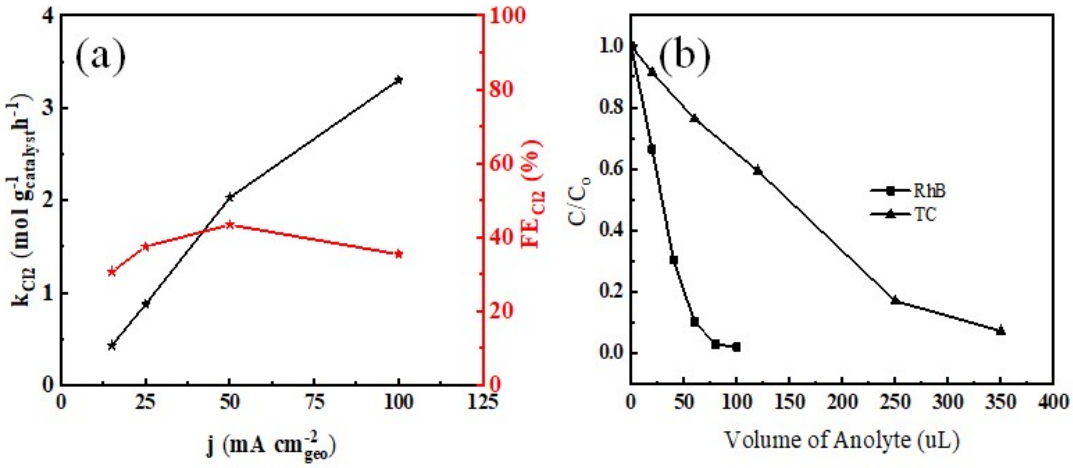

Figure S12. (a) Production rate (left) and Faradaic efficiency (right) of Cl_2 in the anode in a triple-phase flow cell under the flow of O_2 in 0.5M NaCl and (b) electrocatalytic degradation of 1 mL Rhodamine B (RhB, 20 ppm) or tetracycline (TC, 20 ppm) in one minute using different amounts of anolyte after 1 h of electrolysis at 50 mA cm^{-2}.

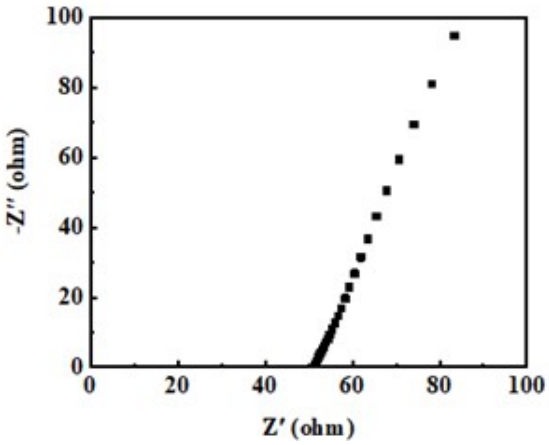

Figure S13. Electrochemical impedance spectroscopy of the flow cell at the open circuit potential.

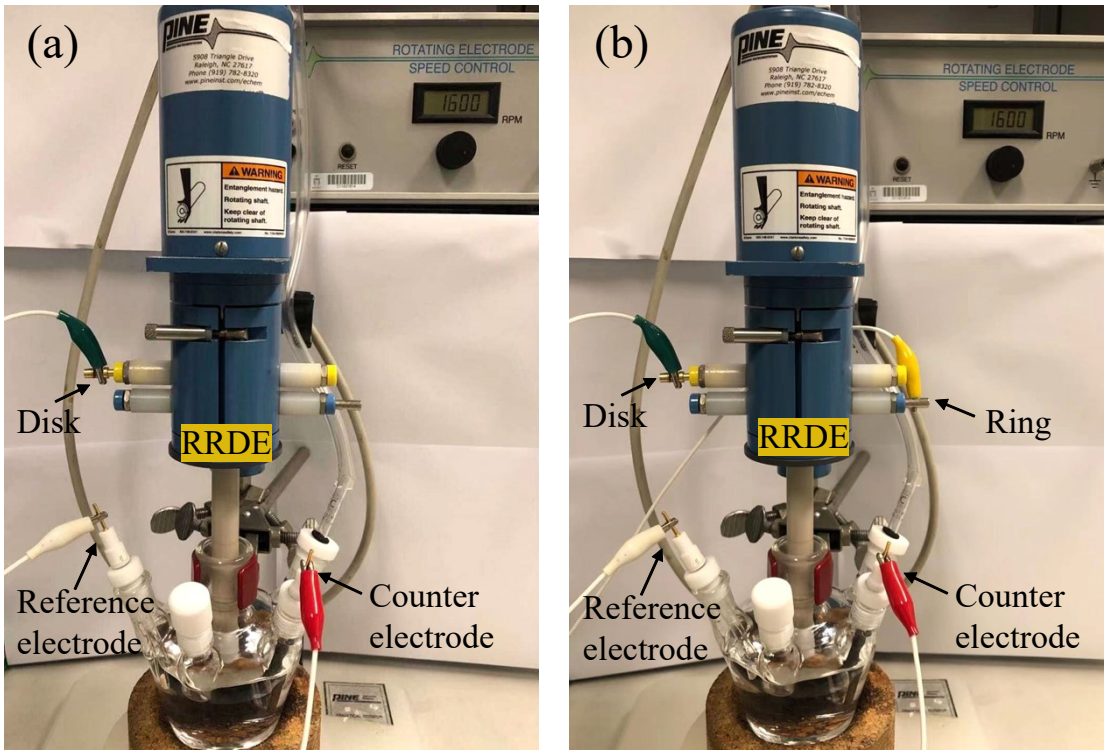

Figure S14. Images of rotating ring-disk electrode (RRDE) setup: (a) the connection to measure disk current only and (b) the connection to measure both disk current and ring current.

Table S4. Comparison of this work and recently reported catalysts for H_2O_2 production via ORR in flow cell.

Catalyst	k_{H2O2} (mol $g^{-1}_{catalyst}$ h^{-1})	FE_{H2O2} (%)	Electrolyte	j (mA cm^{-2})	Ref No. in Figure 4c
Co-N-C	4.5	95.6	0.5M NaCl	50	This work
Co-C	0.056	30	PEM*	30	[50][1]
CB-10%	3.66	~90	SE*	200	[51][2]
NADE	0.227	66.8	0.05M Na_2SO_4	240	[52][3]
CMK3-20s	0.837	78	0.1 M K_2SO_4	~14	[55][4]
CoTPP/KB	0.475	50	PEM*	95	[56][5]
CoTPP/VGCF (1073 K)	0.1458	32	PEM*	80	[57][6]
MnCl-OEP/AC (823 K)	0.018	34.1	0.6 M H_2SO_4	56.1	[53][7]
AC(HNO_3 3.8 M)+VGCF	0.036	31	~0.6 M H_2SO_4	~30	[54][8]
Co-N-C	4.33	50	0.1M KOH	~50	[15][9]
N-FLG-8	3.11	99.8	0.1M KOH	36.1	[58][10]
Ni-N_2O_2	5.9	90	0.1M KOH	70	[20][11]
N-O-P-C-800	0.54	93.1	0.1M KOH	~14	[59][12]
VGCF+XC72	0.0325	94	2M NaOH	100	[60][13]

*PEM: proton exchange membrane with neutral DI water as carrier flow

*SE: solid electrolyte with neutral DI water flow

Reference

1. W. T. Li, A. Bonakdarpour, E. Gyenge and D. P. Wilkinson, *J. Appl. Electrochem.*, 2018, 48, 985-993.
2. C. Xia, Y. Xia, P. Zhu, L. Fan and H. Wang, *Science*, 2019, 366, 226-231.
3. Q. Zhang, M. Zhou, G. Ren, Y. Li, Y. Li and X. Du, *Nat. Commun.*, 2020, 11, 1731.
4. Y.-L. Wang, S.-S. Li, X.-H. Yang, G.-Y. Xu, Z.-C. Zhu, P. Chen and S.-Q. Li, *J. Mater. Chem. A*, 2019, 7, 21329-21337.
5. T. Iwasaki, Y. Masuda, H. Ogihara and I. Yamanaka, *Electrocatalysis*, 2018, 9, 236-242.
6. I. Yamanaka, S. Tazawa, T. Murayama, T. Iwasaki and S. Takenaka, *ChemSusChem*, 2010, 3, 59-62.

7. I. Yamanaka, T. Onizawa, H. Suzuki, N. Hanaizumi, N. Nishimura and S. Takenaka, *J. Phys. Chem. C*, 2012, 116, 4572-4583.
8. T. Murayama and I. Yamanaka, *J. Phys. Chem. C*, 2011, 115, 5792-5799.
9. Y. Sun, L. Silvioli, N. R. Sahraie, W. Ju, J. Li, A. Zitolo, S. Li, A. Bagger, L. Arnarson and X. Wang, *J. Am. Chem. Soc.*, 2019, 141, 12372-12381.
10. L. Li, C. Tang, Y. Zheng, B. Xia, X. Zhou, H. Xu and S. Z. Qiao, *Adv. Energy Mater.*, 2020, 10, 2000789.
11. Y. Wang, R. Shi, L. Shang, G. I. Waterhouse, J. Zhao, Q. Zhang, L. Gu and T. Zhang, *Angew. Chem., Int. Ed.*, 2020, 59, 13057-13062.
12. H.-X. Zhang, S.-C. Yang, Y.-L. Wang, J.-C. Xi, J.-C. Huang, J.-F. Li, P. Chen and R. Jia, *Electrochim. Acta*, 2019, 308, 74-82.
13. I. Yamanaka, *Catal. Surv. Asia*, 2008, 12, 78-87.